ARTICLE
Journal of Cellular Biochemistry 108:1376–1388 (2009)

Journal of Cellular Biochemistry

Proteomic Analysis of Differentially Expressed Proteins in Human Cholangiocarcinoma Cells Treated with *Clonorchis sinensis* Excretory–Secretory Products

Jhang Ho Pak,[1*] Ju Hyun Moon,[1] Seung-Jun Hwang,[2] Shin-Hyeong Cho,[3] Sang-Beom Seo,[4] and Tong-Soo Kim[5**]

[1]*Asan Institute for Life Sciences, University of Ulsan College of Medicine, Asan Medical Center, Seoul 138-736, South Korea*

[2]*Department of Anatomy and Cell Biology, University of Ulsan College of Medicine, Asan Medical Center, Seoul 138-736, South Korea*

[3]*Division of Malaria and Parasitic Diseases, National Institute of Health, Seoul 122-701, South Korea*

[4]*Deptartment of Life Science, College of Natural Sciences, Chung-Ang University, Seoul 156-756, South Korea*

[5]*Deptartment of Parasitology, Inha University School of Medicine, Inchon 400-103, South Korea*

ABSTRACT

Severe *Clonorchis sinensis* infection is a significant risk factor for malignant changes in bile ducts and surrounding liver tissues occurring as a result of direct contact with *C. sinensis* worms and their excretory–secretory products (ESP). However, the intrinsic molecular mechanisms involved in these processes remain obscure. To determine the effects of *C. sinensis* infection on protein expression in host bile duct epithelium, we examined proteomic profile changes in the human cholangiocarcinoma cell line (HuCCT1) treated with ESP at 24 h. Using a combination of 2-DE, quantitative image and MALDI-TOF MS analysis, we identified 83 proteins that were translationally modulated in response to ESP, among which 49 were up-regulated and 34 down-regulated. These proteins were classified under various biological categories, including metabolism, cell structure and architecture, proteolysis, protein modification, transport, signal transduction, and reactive oxygen species (ROS) detoxification. In particular, ESP induced the expression of redox-regulating proteins, including peroxiredoxins (Prdx 2, 3, and 6) and thioredoxin 1 (Trx 1), possibly via intracellular ROS generation. Application of the proteomic approach to identify ESP response proteins should be a prerequisite before further investigation to clarify the molecular pathways and mechanisms involved in *C. sinensis* infection of host cells. J. Cell. Biochem. 108: 1376–1388, 2009.

KEY WORDS: *Clonorchis sinensis*; EXCRETORY–SECRETORY PRODUCTS; HUMAN CHOLANGIOCARCINOMA CELLS (HuCCT1); PEROXIREDOXIN; 2-DE-BASED PROTEOMICS

Human clonorchiasis is caused by infection of the Chinese or oriental liver fluke, *Clonorchis sinensis*, which is widely distributed in Eastern Asian countries, including Korea, China, Taiwan, and Northern Vietnam. More than 7 million people are infected in these areas through ingestion of uncooked freshwater fish containing *C. sinensis* metacercariae. The metacercariae excyst in the host's duodenum, juvenile flukes migrate to the ampulla of Vater, and ascend into the bile ducts where they grow into adult worms. They reside in the peripheral small bile ducts for a long period, and induce chronic inflammation, dilatation, mechanical

Abbreviations used: ESP, excretory–secretory products; 2-DE, two-dimensional gel electrophoresis; GAPDH, glyceraldehyde-3-phosphate dehydrogenase; NAC, *N*-acetylcysteine; Prdx, peroxiredoxin; ROS, reactive oxygen species; Trx, thioredoxin; TUNEL, terminal deoxynucleotidyl transferase-mediated dUTP nick end labeling; VCP, valosin-containing protein.

Grant sponsor: National Institute of Health, Ministry of Health and Welfare, Korea; Grant number: 2008-E00272-00; Grant sponsor: Asan Institute for Life Sciences, Seoul, Korea; Grant number: 2007-349.

*Correspondence to: Prof. Jhang Ho Pak, Asan Institute for Life Sciences, University of Ulsan College of Medicine, Asan Medical Center, 388-1 Pungnap-2 dong, Songpa-gu, Seoul 138-736, South Korea. E-mail: jhpak@amc.seoul.kr

**Correspondence to: Tong-Soo Kim, Department of Parasitology, Inha University School of Medicine, Shinheung-dong, Choong-gu, Inchon 400-712, South Korea. E-mail: tongsookim@inha.ac.kr

Received 26 June 2009; Accepted 3 September 2009 • DOI 10.1002/jcb.22368 • © 2009 Wiley-Liss, Inc.
Published online 1 October 2009 in Wiley InterScience (www.interscience.wiley.com).

obstruction, and bile duct wall thickening, leading to increased risk of malignancy in the bile duct and surrounding liver tissue [Crompton, 1999; Rim, 2005]. While clonorchiasis is asymptomatic in most cases, severe and chronic infections may be complicated by cholangitis, cholelithiasis, cholangiectasis, and even cholangiocarcinoma. In particular, carcinogenesis associated with clonorchiasis may result from chronic irritation and prolonged inflammation of the bile duct epithelium and bile contamination as a result of direct contact with *C. sinensis* worms and their secretion products [Watanapa and Watanapa, 2002]. Hospital-based case studies reveal a high incidence of concurrent intra- and extra-hepatic cholangiocarcinoma and clonorchiasis in areas endemic to *C. sinensis* [Papachristou et al., 2005; Choi et al., 2006], although the mechanisms involved remain to be established.

Similar to other parasitic helminths, *C. sinensis* continuously releases excretory–secretory products (ESP) into its extracellular environment during host infection. ESP are predominantly composed of various proteins, some of which immunoreact with the sera of *C. sinensis*-infected patients [Hong et al., 2002; Kang et al., 2004; Li et al., 2004; Pak et al., 2009]. Proteome profiles have been analyzed from *Fasciola hepatica* and *C. sinensis* adult worm ESP [Jefferies et al., 2001; Ju et al., 2009]. The most prominent proteins identified from both ESP are proteases and detoxicating enzymes, which may protect parasites from host immune response. Cells exposed to liver fluke ESP display diverse physiologic responses, depending on the cell type. For example, ESP from *C. sinensis* and *Opisthorchis viverrini* stimulate proliferation in HEK293 and NIH/3T3 cells via induction of E2F1 transcription factor and cell cycle regulatory proteins, respectively [Thuwajit et al., 2004; Kim et al., 2008]. On the other hand, treatment with *F. hepatica* ESP inhibits proliferative responses to mitogens in rat splenocytes [Cervi and Masih, 1997] and causes apoptotic cell death in rat eosinophils via activation of tyrosine kinases and the caspase cascade [Serradell et al., 2007]. These studies suggest that ESP from the liver flukes play pivotal roles in pathologic processes, such as development of cholangiocarcinoma and immunosuppression.

In view of the above findings, it is of significant interest to explore the global changes in gene/protein expression involved in *C. sinensis* ESP-mediated molecular mechanisms in host cells. We previously profiled differentially expressed genes in a human cholangiocarcinoma cell line (HuCCT1) treated with *C. sinensis* ESP using cDNA microarray analysis, which were consistently increased/decreased by at least twofold relative to the untreated control between 1 and 24 h. Up-regulated genes were involved in the development of carcinogenesis, whereas down-regulated genes participated in apoptosis [Pak et al., 2009].

In the present study, we apply the proteomic approach to investigate translational responses in ESP-exposed HuCCT1 cells. Proteomic analysis is a useful tool for detecting significant changes in protein expression of two or more samples and identifying target proteins with no prior knowledge of signaling pathways in the cells [Blacktock and Weir, 1999]. To establish differences in expression between ESP-treated and untreated cells, phenotyping was accomplished using a combination of 2-DE, quantitative image analysis of fractionated proteins, and MALDI-TOF MS analysis. We identified 83 regulated proteins in HuCCT1 cells in response to ESP, with a view to clarifying the mechanisms of host cell response. Specifically, the levels of peroxiredoxin (Prdx) isoforms (Prdx 2, 3, and 6) and thioredoxin 1 (Trx 1) were highly elevated, probably as a consequence of intracellular reactive oxygen species (ROS) generation, although we cannot exclude the possibility of participation of additional signals for Prdx 3 induction. We discuss the possible roles of these proteins in connection with ESP as a potential carcinogen.

MATERIALS AND METHODS

MATERIALS

All cell culture media components were purchased from Life Technologies (Gaithersburg, MD). IPG strips (Immobiline DryStrip, 0.5 mm × 3 mm × 180 mm, pH 4–7, 4.5–5.5, and 5.5–6.7), Dithiothreitol (DTT), urea, CHAPS, Ready Sol IEF 40% solution, and IPG buffers were purchased from GE HealthCare Biosciences (Uppsala, Sweden). Silver nitrate was obtained from Fluka Chemie (Seinheim, Switzerland) and sequencing grade trypsin from Roche Diagnostics (Mannheim, Germany). All other chemicals and reagents were acquired from Sigma–Aldrich (St. Louis, MO) or Merck (Whitehouse Station, NJ), unless otherwise indicated.

PREPARATION OF *C. sinensis* ESP

Metacercariae of *C. sinensis* were collected from naturally infected freshwater fish, *Pseudorasbora parva*, in an endemic area of Korea. New Zealand albino rabbits weighing 1.5–2 kg were orally infected with 500 metacercariae each, and euthanized 8 weeks later. Isolation of adult worms from bile ducts and ESP collection were performed as described previously [Pak et al., 2009]. ESP was concentrated with Centriprep YM-10 (Millipore, Bedford, MA), followed by filtering through a 0.2 μm syringe filter. Protein concentrations were measured using a Protein Assay Kit (Bio-Rad, Hercules, CA), and ESP were stored in aliquots at −80°C until use.

CELL CULTURE AND ESP TREATMENT

HuCCT1 cells were cultured in RPMI 1640 medium supplemented with 10% fetal bovine serum (FBS) and an antibiotic mixture at 37°C in humidified 5% CO_2. Cells were seeded at a density of 5×10^6 or 3×10^5 cells in a 150 or 35 mm culture plate, and grown for 24 h under standard conditions. To avoid possible serum effect, cells were gradually deprived of serum by incubation in 1% FBS overnight, followed by incubation in serum-free medium for 3 h. Serum-starved cells were treated with 800 ng/ml ESP and incubated for the indicated times.

SAMPLE PREPARATION AND TWO-DIMENSIONAL POLYACRYLAMIDE GEL ELECTROPHORESIS

Cells were treated with 800 ng/ml ESP or equal volumes of PBS as a control for 24 h. Cell extracts for 2-DE were prepared according to previous reports [Shim et al., 2004; Park et al., 2006; Shim et al., 2006]. We analyzed at least three independent sets of cultures, which were assessed for proteomic changes, based on similar 2-DE conditions.

PROTEIN VISUALIZATION AND IMAGE ANALYSIS

Gels were silver-stained, as described previously [Yan et al., 2000]. Briefly, gels were fixed with methanol:acetic acid:water (40:10:50, v/v/v), and sensitized in 30% methanol, 5% sodium thiosulfate, 6.8% (w/v) sodium acetate. After washing in deionized water, proteins were stained with 2.5% silver nitrate, followed by a second wash in deionized water. Subsequently, gels were developed with 2.5% (w/v) sodium carbonate, 0.04% formaldehyde. Once the desired intensity was attained, the developing process was stopped with 1.46% (w/v) EDTA solution. Protein patterns in gels were scanned and analyzed using GS-800 Calibrated Imaging Densitometer (Bio-Rad) and the Melanie IV 2-DE software package (Geneva Bioinformatics S.A., Geneva, Switzerland), respectively. For account of experimental variations and comparison between ESP- and PBS-treated samples, three gels of each group were prepared and a match set was created from protein patterns of each three gels, thus obtaining one ''average map'' for each group. Spot quantities of all gels were normalized, rendering that the volume of each spot density in a gel was divided by the total volumes of all spot densities in that gel. Statistical analysis of Melanie IV allowed the detection of proteins that were differentially regulated by ESP.

IN-GEL DIGESTION

Protein spots of interest were manually excised from the gel and placed in Eppendorf tubes. Gel pieces were destained in a 1:1 mixture of 30 mM potassium ferricyanide and 100 mM sodium thiosulfate, washed with 50% ACN/25 mM ammonium bicarbonate, pH 7.8, and incubated in 50% ACN for 5 min. Gel pieces were dehydrated in a vacuum centrifugal concentrator and incubated in 10 μl of trypsin (0.02 μg/μl) solution on ice for 45 min. After replacing with 20 mM ammonium carbonate, gel pieces were digested at 37°C overnight. The following day, 0.5% (v/v) TFA in 50% ACN was added, and the extraction conducted twice in an ultrasonic water bath. Peptides were extracted in 0.1% formic acid in 2% ACN for further MALDI-TOF MS analysis.

MALDI-TOF MS ANALYSIS AND DATABASE SEARCH FOR PROTEIN IDENTIFICATION

Mass analysis was performed on a PerSeptive Biosystem Voyager-DE STR™ MALDI-TOF MS (Applied Biosystems, Foster City, CA) in a reflector mode for positive ion detection. Peptide extracts were dispensed on to a MALDI sample plate, along with matrix solution consisting of 10 mg/ml α-cyano-4-hydroxycinnamic acid, 0.1% TFA and 50% ACN. External peptide calibrants, angiotensin I (monoisotopic mass, 1296.6853), rennin substrate (1758.9331) and adrenocorticotropic hormone (2465.1989) were employed for mass calibration. Spectra were internally calibrated using autolytic fragments from trypsin. For each sample, 18–20 spectra were acquired in the delayed extraction and reflector mode, carefully observed, and the contaminant peak masses were eliminated. Proteins were identified by peptide mass fingerprinting with the search engine program, ProFound. The criteria for positive identification of proteins were set as follows: (i) at least 4 matching peptide masses, (ii) 50 ppm or better mass accuracy, and (iii) matching of M_r and pI of identified proteins with the values estimated from image analysis.

IMMUNOBLOT ANALYSIS

A number of differentially expressed proteins were validated by immunoblot analyses using commercially available target specific antibodies. Total cell lysates/lane (30 μg) were size-fractionated using 7–14% gradient SDS–PAGE. Proteins were electrophoretically transferred onto nitrocellulose membranes (Schleicher & Schull, Dassel, Germany) using a Semi-Dry Transfer Blotter (GE HealthCare), and subsequently probed with corresponding primary antibodies to target proteins (annexin I, calpain, valosin-containing protein [VCP] and cathepsin D from Santa Cruz Biotechnology [Santa Cruz, CA], Trx 1 and Prdx 1-6 from AbFrontier Co. [Seoul, Korea]). After incubating with horseradish-peroxidase-conjugated host specific anti-IgGs (Jackson ImmunoResearch Laboratory, West Grove, PA), the reaction was detected with enhanced chemiluminescence (ECL; GE HealthCare) and quantitated by densitometric scanning of the X-ray film with a FluorS Multi-Imager (Bio-Rad). To normalize for protein loading, blots were washed in BlotFresh Western Blot Stripping Reagent (SignaGen Laboratories, Gaithersburg, MD) according to the manufacturer's instructions, and reprobed with a monoclonal antibody to β-actin (Sigma–Aldrich).

TOTAL RNA EXTRACTION AND RT-PCR ANALYSIS

Total RNA was isolated from cells using an RNeasy Mini Kit (Qiagen, Valenica, CA), and RT-PCR was performed according to the manufacturer's instructions (SuperScript II First-strand, Invitrogen, Carlsbad, CA; ExTaq, TaKaRa Bio, Inc., Shiga, Japan). The reaction conditions were as follows: 25–30 cycles of denaturation at 95°C for 45 s, annealing at 55°C for 45 s, extension at 72°C for 45 s, and a final cycle at 72°C for 2 min. Table I presents a pair of primers designed with the PrimerDesigner program, based on the cDNA sequences of each human Prdx isoform and glyceraldehyde-3-phosphate dehydrogenase (GAPDH) in the GeneBank database. PCR products were separated on 1.2% agarose gels, and images were captured for quantitation of DNA band densities.

CELL PROLIFERATION AND APOPTOSIS

Cell proliferation in response to ESP was evaluated with a colorimetric Cell Counting Kit-8 (CCK-8; Dojindo Laboratories, Kumamoto, Japan) according to the manufacturer's instructions. Cells were seeded at a density of 2×10^3 cells/well in a 96-well plate and treated with 800 ng/ml ESP for 24 or 48 h, as described above. The amount of formazan dye generated from cellular dehydrogenase activity was measured by absorbance at 450 nm using a microplate spectrophotometer (Molecular Devices Corp., Sunnyvale, CA). Absorbance values were converted to percentages for comparison with the untreated control.

Apoptosis was evaluated with an in situ cell death detection kit, TMR Red (Roche Diagnostics, Mannheim, Germany), according to the manufacturer's instructions. After terminal deoxynucleotidyl transferase-mediated dUTP nick end labeling (TUNEL) reaction, cells were evaluated using a fluorescence microscope with the proper filter. For each experiment, the percentage of TUNEL-positive cells was determined by counting ~500 cells per dish from five to six randomly selected fields.

TABLE I. Primer Sequences of Prdx Isoforms and GAPDH for RT-PCR

Gene	Primer sequence	Acc. No.	Product size (bp)
Pdrx 1	Forward: 5′-CAAAGCCACAGCTGTTATGC-3′ Reverse: 5′-TCCCCATGTTTGTCAGTGAA-3′	NM_002574	468
Prdx 2	Forward: 5′-TCAAAGAGGTGAAGCTGTCG-3′ Reverse: 5′-ACGTTGGGCTTAATCGTGTC-3′	NM_181738	487
Prdx 3	Forward: 5′-GCCGTTGTCAATGGAGAGTT-3′ Reverse: 5′-TAGGAGAATCCGGTGTCCAG-3′	NM_014098	490
Prdx 4	Forward: 5′-CAGCTGTGATCGATGGAGAA-3′ Reverse: 5′-GGCAGACTTCTCCGTGTTTG-3′	NM_006406	465
Prdx 5	Forward: 5′-ACGGTGCAGTGAAGGAGAGT-3′ Reverse: 5′-AAGATGGACACCAGCGAATC-3′	NM_181651	426
Prdx 6	Forward: 5′-CCTGGAGCAAGGATATCAAT-3′ Reverse: 5′-GTCAGCTGGAGAGAGATGAC-3′	NM_004905	574
GAPDH	Forward: 5′-ACCCAGAAGACTGTGGATGG-3′ Reverse: 5′-CAGGAAATGAGCTTGACAAAG-3′	NM_002046	389

DETECTION OF INTRACELLULAR REACTIVE OXYGEN SPECIES

Intracellular generation of reactive oxygen species (ROS) was detected using 2′,7′-dichlorodihydrofluorescein diacetate (CM-H_2-DCFDA; Molecular Probes, Inc., Eugene, OR). Cells grown on aclar plates or 96-well plates were incubated in phenol red-free medium containing 400–1,600 ng/ml ESP for the indicated times with or without *N*-acetylcysteine (NAC). Cells were washed once in Hank's balanced salt solution (HBSS), and loaded with 10 μM CM-H_2DCFDA for 30 min at 37°C. After washing with HBSS, cells on aclar plates were fixed with 4% paraformaldehyde, air-dried, and inversely applied to slides with mounting solution. Fluorescence images were captured using a fluorescence microscope with a single rapid scan and identical parameters for different intensity detection. Intracellular levels of DCF fluorescence were measured using a microplate spectrofluorometer (Molecular Devices Corp.), with excitation at 485 nm and emission at 538 nm. Background fluorescence in wells without cells was subtracted from all other values. Values were converted to percentages for comparison with the untreated control.

STATISTICAL ANALYSES

Data are expressed as means ± SEs for three or more independent experiments. Statistical significance was evaluated by one-way analysis of variance (ANOVA), followed by Student's *t*-test or Bonferroni's test, as appropriate. Differences in mean values were considered statistically significant at $P < 0.05$.

RESULTS

ESTABLISHMENT OF *C. sinensis* ESP-INDUCED CONDITIONS

We previously established the appropriate *C. sinensis* ESP concentration (800 ng/ml) and incubation times (between 1 and 24 h) at which significantly regulated genes in HuCCT1 cells were detected [Pak et al., 2009]. As shown in Figure 1, these conditions do not significantly affect proliferation or apoptosis, which may lead to regulation of the related proteins. At 48 h of incubation, cell viability decreased by ~7.6% and TUNEL-positive cells increased by ~4.1%. This finding may be attributed to prolonged serum starvation, since apoptotic rate of 48 h PBS-treated cells was not statistically significant compared with that of 48 h ESP-treated cells (~3.7%, $P > 0.05$; Fig. 1B), also both rates remained essentially unchanged even under higher ESP concentrations (1,600 ng/ml; data not shown). As a result, subsequent proteomic analyses were limited to 800 ng/ml ESP and the initial 24 h period before the commencement of extensive cell death, which may lead to masking of actual ESP-dependent changes in protein expression, making the results difficult to interpret.

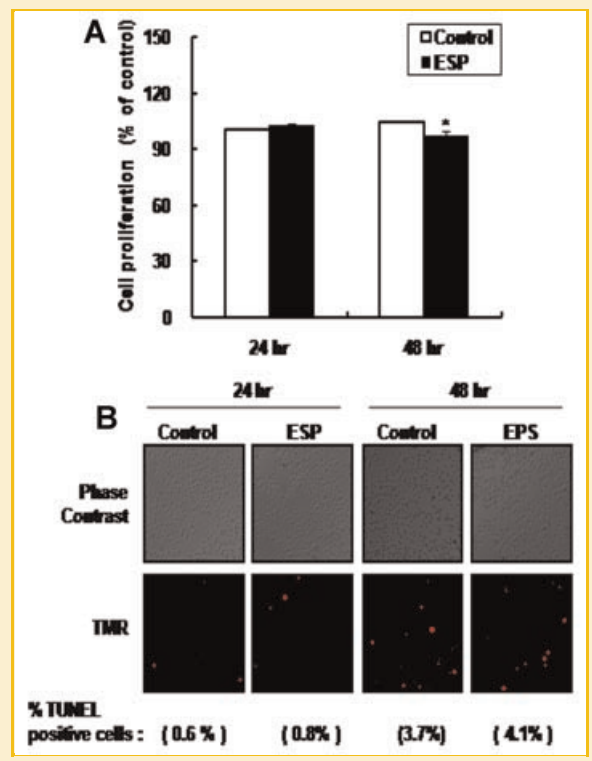

Fig. 1. Effects of ESP on HuCCT1 cell proliferation and apoptosis. Cells were treated with 800 ng/ml ESP or an equal volume of PBS (untreated control) for 24 and 48 h. A: Cell proliferation was measured based on formazan dye production in a CCK-8 assay. Each dataset represents a relative percentage of the control. Data are presented as means ± SE of three independent experiments. *$P < 0.05$ compared with the 48 h control. B: Fluorescence staining for nuclear DNA fragmentation was detected with the TUNEL assay. The percentage of TUNEL-positive cells was determined from ~500 cells in five to six microscopic fields.

PROTEOME PROFILE OF ESP TREATED VERSUS UNTREATED CELLS

High-resolution 2-DE is a useful technique to fractionate protein mixtures from various tissues and cells. The majority of protein spots in general mammalian cells are clustered within a pI range of 4–7 [Shim et al., 2004, 2006; Park et al., 2006]. Accordingly, we employed the 2D gel system composed of immobilized pH gradients as the first dimension (pH ranges of 4–7, 4.5–5.5, or 5.5–6.7) and 7–14% linear gradient SDS–PAGE as the second dimension, followed by silver staining. To account for experimental variations, more than three gels were prepared for both 24 h PBS- and ESP-treated cells cultured with the same schedules under similar conditions. We detected approximately 1,300 separable protein spots at pH 4–7, 1,250 at pH 4.5–5.5, and 900 at pH 5.5–6.7 in both samples. Quantification of the staining volumes of individual spots revealed that the majority of total spots on each pH gradient gel were similar, regardless of ESP treatment. To further identify proteins that were expressed differentially in the presence of ESP, we selected 50 spots on each gel that remained unchanged between the two groups for normalization. Spots were identified by MALDI-TOF MS analysis, and compared with the database from the ProFound Search Engine. The gel positions of the fourteen reference proteins at pH 4–7 are shown in Figure 2 with identification. These spots provided a reference framework for comparison of M_r and pI observed on gel migration. Theoretical values calculated from the amino acid sequences and the observed values were very similar in most cases. The results indicate that the complex protein mixtures in both samples are well dissolved in our 2-DE system, allowing the analysis of subsequent ESP-mediated differential protein expression in HuCCT1 cells.

IDENTIFICATION OF DIFFERENTIALLY EXPRESSED PROTEINS IN ESP-TREATED CELLS

The differences in spot intensities between PBS- and ESP-treated proteins were compared visually and evaluated with Melanie IV image analysis software. To obtain qualitative and reproducible results, we analyzed more than three gels for each proteome profile, and selected those with similar normalized protein volumes. After gel-to-gel matching and normalization, we observed altered relative staining intensities of 292 protein spots (75 spots on the pH 4–7 gel, 115 spots on the pH 4.5–5.5 gel, and 102 spots on the pH 5.5–6.7 gel) in ESP-treated cells, compared with untreated control. Spots exhibiting at least a 2.5-fold difference in volume based on expression were excised and subjected to in-gel trypsin digestion, leading to the successful identification of 83 proteins using MALDI-TOF MS and peptide fingerprinting analyses. Among the 83 proteins, 32 were identified in the pH 4–7 gel (9 down-regulated and 23 up-regulated), 25 at pH 4.5–5.5 (3 down-regulated and 22 up-regulated, three of which were identical to those in the pH 4–7 gel), and 30 at pH 5.5–6.7 (22 down-regulated and 8 up-regulated, one of which was identical to that in the pH 4–7 gel). The results indicate that ESP influences the changes in expression patterns of various host cellular proteins. As an example, we present two magnified areas of each pH range gel showing three proteins down- or up-regulated by ESP (Fig. 3).

To clarify the biological significance of the differentially expressed proteins, MS-identified proteins at each pH range were classified into functional groups using the Panther database. Protein designations and properties are summarized in Table II. In general, the major clustered groups comprised 49 proteins playing roles in metabolism, proteolysis, cell structure and architecture, signaling,

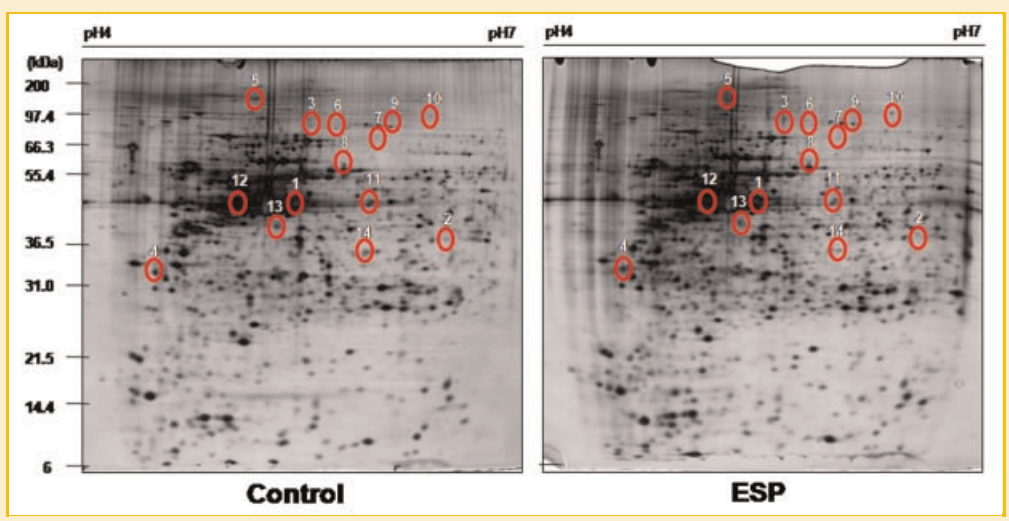

Fig. 2. Representative 2-DE gel patterns of 24 h PBS- (control) and ESP-treated (ESP) HuCCT1 cells at pH ranges of 4–7. For 2-DE, 350 μg of total proteins were applied by in-gel rehydration to IPG strips, followed by 7–14% gradient SDS–PAGE for the second dimension. Gels were visualized by silver staining. Fourteen identified reference proteins are marked as numbers on both gels; (1) ACTB protein (β-actin), (2) Macrophage-capping protein, (3) Heat shock 70 kDa protein 4L, (4) Prohibitin 2, (5) Neutral α-glucosidase AB isoform 2, (6) Hypothetical protein, (7) Heat shock 70 kDa protein 9 (mortalin), (8) Unnamed protein product, (9) Inner membrane protein, mitochondrial isoform 2, (10) Mitochondrial matrix protein P1, (11) Serine proteinase inhibitor, clade A, member 1, (12) Protein disulfide isomerase-related protein 5, (13) Paraoxonase 2 isoform 1, and (14) Unnamed protein product.

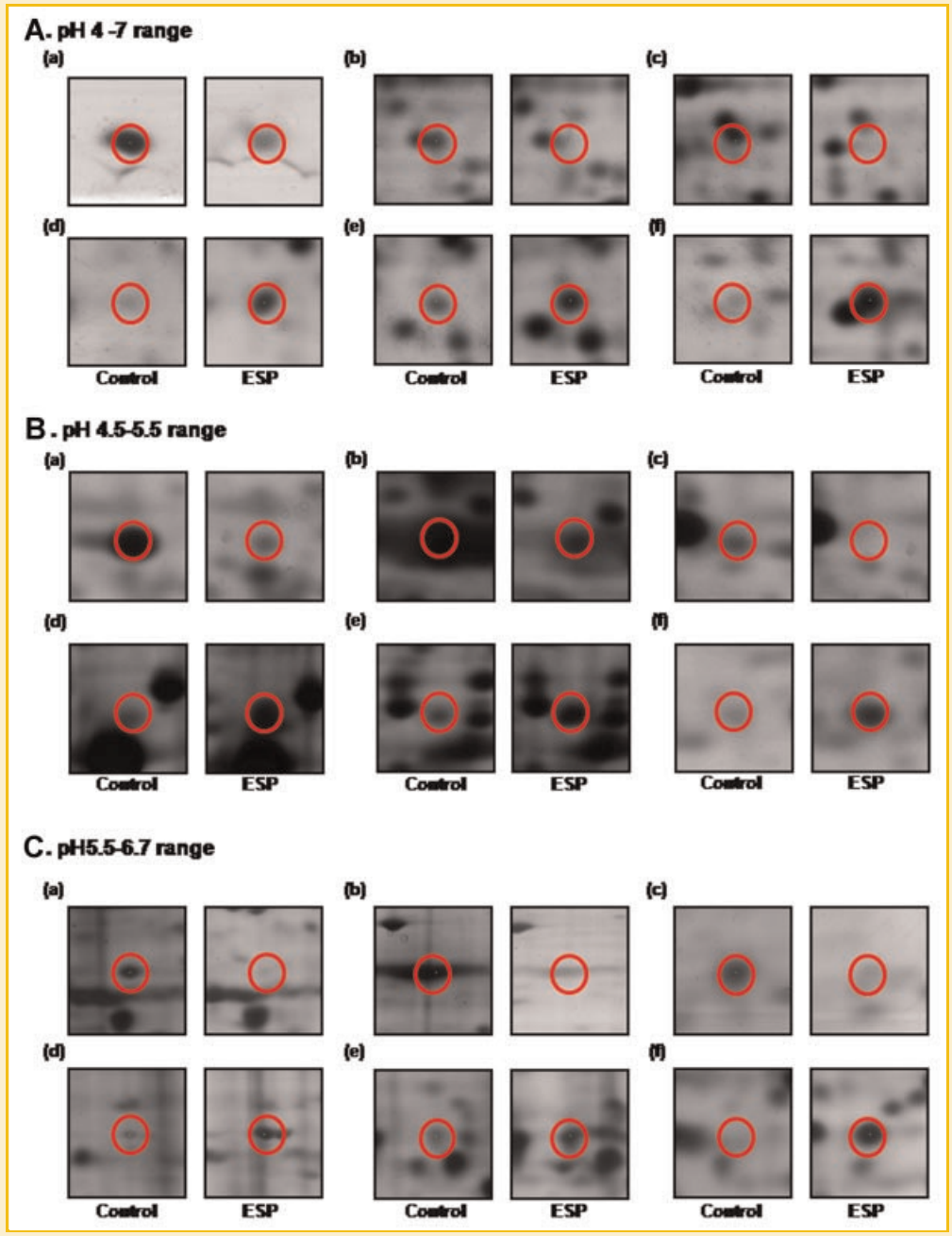

Fig. 3. Magnified regions of comparative protein spots between 24 h PBS- (control) and ESP- treated (ESP) cells at different pH ranges. The 2-DE pattern of control is on the left and ESP on the right. The down-regulated (a–c) and up-regulated protein spots (d–f) are displayed as magnified regions from the gel. A: 2-DE gel at pH 4–7 (a) Barrier to autointegration factor 1, (b) MutL homolog 3 (*E. coli*), (c) Heterogeneous nuclear ribonucleoprotein H1, (d) Stratifin, (e) Proteasome α5 subunit, and (f) PDZ and LIM domain protein 1. B: 2-DE gel at pH 4.5–5.5 (a) Heterogeneous nuclear ribonucleoprotein K, (b) Endozepine-related protein, (c) Keratin 19, (d) Proteasome subunit Y, (e) Tetraspan TM4SF, and (f) Triosephosphate isomerase 1. C: 2-DE gel at pH 5.5–6.7 (a) Lamin, (b) Filamin Aα, (c) Chromosome 1 open reading frame 124, (d) Lamin A/C isoform 1 precursor, (e) Glucose 6-phosphate dehydrogenase isoform α, and (f) Annexin 1.

transport, translation, and immune responses. While 18 proteins remained functionally unclassified, 16 proteins were involved in mRNA splicing, protein targeting, stress response, antioxidation, transcription, protein modification/phosphorylation, meiosis, and cytokinesis. These results indicate that ESP stimulates significant changes in host cellular proteins involved in various biological processes.

To validate the differential expression patterns of the identified candidates, we performed immunoblot analysis of annexin 1, cathepsin D, calpain, and valosin-containing protein (VCP) displaying up-regulated expression at 24 h ESP exposure. These proteins were selected because they were identified at each pH range tested and their specific antibodies are commercially available. We examined differential expression patterns between

TABLE II. MS-Identified Proteins in Cells Treated With ESP for 24 h Versus Untreated Control

Protein identified	Swiss-Prot/ NCBI Acc. No.	pI	M_r	Z score	Seq. Cov. (%)	Up (U) or down (D)
(A) pH range of 4–7 metabolism						
Metabolism						
Tigger transposable element derived 4	NP_663772	6	58.3	1.86	9	D
Enolase 1 (α)	NP_001419	6.6	40.92	2.43	21	D
Enolase 2	NP_001966	4.9	47.68	2.43	22	U
Exosome component 7	NP_055819	5.1	32.47	2.43	27	U
Valosin-containing protein	NP_009057	6.1	34.8	1.69	18	U
Triosephosphate isomerase 1	NP_000356	6.5	26.88	2.43	34	U
Catabolism						
Pyrophosphatase 1	NP_066952	5.5	33.21	2.32	28	U
Cell structure and architecture						
PDZ and LIM domain protein1	NP_066272	6.6	36.62	2.43	14	U
Tubulin α 6	NP_116093	5	50.73	1.97	29	U
Tubulin β	NP_821133	4.2	14.47	2.07	15	U
Proteolysis						
Cathepsin D preproprotein	NP_001900	6.1	45.17	1.77	18	U
Cathepsin B preproprotein	NP_001899	5.2	5.2	2.43	21	D
Proteasome α5 subunit	NP_002781	4.7	26.61	2.43	36	U
mRNA splicing						
Heterogeneous nuclear ribonucleoprotein H1	NP_005511	5.9	49.57	1.93	23	D
Breast carcinoma amplified sequence 2	NP_005863	5.5	26.26	1.84	21	D
Signaling						
Progesterone receptor membrane component 1	NP_006658	4.5	21.8	1.89	13	U
Rho GDP dissociation inhibitor (GDI) α	NP_004300	5	23.26	2.3	48	U
EGF-containing fibulin-like extracellular matrix protein 2	NP_058634	4.8	51.74	1.93	14	U
Stratifin	NP_006133	4.8	24.39	2.43	57	U
Transport						
Chloride intracellular channel 1	NP_001279	5	27.33	2.43	39	U
Protein targeting						
Tyrosine 3-monooxygenase/tryptophan 5-monooxygenase activation protein, γ polypeptide	NP_036611	4.8	28.5	2.43	30	U
Translation						
Eukaryotic translation elongation factor 1 δ isoform 2	NP_001951	4.9	31.25	2.43	31	U
Stress response						
Stress-induced-phosphoprotein 1 (Hsp70/Hsp90-organizing protein)	NP_006810	6.4	63.4	1.77	17	U
Antioxidation						
Peroxiredoxin 6	NP_004896	6	25.16	1.96	39	U
Defense and immunity						
Major histocompatibility complex, class I, B precursor	NP_005505	5.7	34.89	2.43	21	U
Protein phosphorylation						
Protein phosphatase 1H (PP2C domain containing)	NP_065751	6.1	47.82	1.89	18	U
Meiosis						
mutL homolog 3 isoform 2	NP_055196	5.8	44.58	1.67	18	D
Unclassified biological function						
Spermatid associated	NP_689932	6.7	52.05	2.43	16	D
Hypothetical protein (integrator complex subunit 3)	NP_075391	5.6	119.86	2.43	8	D
Barrier to autointegration factor 1	NP_003851	5.8	10.32	1.67	44	D
Laminin-binding protein (Ribosomal protein SA)	NP_002286	4.8	31.92	2.43	26	U
ZNF777 protein (zinc finger protein 77)	NP-056509	6.5	60.77	2.43	14	U
(B) pH range of 4.5–5.5						
Metabolism						
Triosephosphate isomerase 1	NP_000356	5.2	19.07	2.01	33	U
nucleophosmin 1 isoform 2	NP_954654	4.6	32.77	2.43	9	U
Proteolysis						
Caspase 8 (apoptosis-related cysteine peptidase)	NP_203519	5	56.31	1.89	11	U
Calpain, small subunit 1	NP_001740	5	28.51	2.43	30	U
Proteasome β 6 subunit	NP_002789	4.8	25.58	2.43	36	U
Cell structure and architecture						
Keratin 19	NP_002267	5	44.09	2.43	21	D
Tubulin α 6	NP_116093	5	50.73	2.43	25	U
Gesolin (scinderin isoform 2)	NP_149119	5.5	81.04	2.43	11	U
Type II keratin subunit protein	NP_006112	5.3	52.98	1.69	18	U
Tropomyosin 3	NP_689476	4.7	27.44	2.43	28	U
Signaling						
Natural killer-associated transcript 2a protein	NP_055326	6.4	27.67	1.81	25	U
Transport						
Endozepine-related protein	NP_663736	5	46.44	2.43	10	D
Translation						
Eukaryotic translation elongation factor 1 δ isoform 2	NP_001951	4.9	31.25	2.43	39	U
Transcription						
Heterogeneous nuclear ribonucleoprotein K	NP_112552	5.4	42.07	2.43	32	D
Muscle development						
EF-hand domain family, member D2	NP_077305	5.2	26.82	1.94	33	U
Antioxidation						
Thioredoxin	NP_003320	4.8	12.07	1.67	30	U

TABLE II. (*Continued*)

Protein identified	Swiss-Prot/ NCBI Acc. No.	pI	M_r	Z score	Seq. Cov. (%)	Up (U) or down (D)
Immune response						
T cell receptor α chain AV12S1 J29 AC	AA074612	5.3	31.12	1.77	26	U
Immunoglobulin heavy chain variable region	AAR32433	4.5	16.33	1.77	23	U
Unclassified biological function						
Nuclear calmodulin binding protein	NP_867209	5.3	73.04	1.68	13	U
Golgi reassembly stacking protein 2	NP_056345	4.7	47.34	2.43	15	U
Tetraspan TM4SF; Tspan-1	NP_005718	4.8	27.07	2.43	21	U
Putative c-Myc-responsive isoform 1	NP_006434	5	19.23	1.7	25	U
Canopy 2 homolog	NP_055070	4.8	21.06	2.35	60	U
Chromosome open reading frame 59	NP_060377	5	17.9	1.96	33	U
RAB GTPase activating protein 1-like isoform A	NP_055672	5.2	93.63	2.43	7	U
(C) pH range of 5.5–6.7						
Metabolism						
Adenosylmethionine decarboxylase 1	NP_001625	5.7	38.82	2.43	21	D
Transcobalamin II	NP_000346	6.4	47.97	2.43	15	D
Isocitrate dehydrogenase 3 (NAD+) α precursor	NP_005521	6.5	40.14	1.85	21	D
DEAD (Asp-Glu-Ala-Asp) box polypeptide 4	NP_077726	5.6	80.36	2.43	19	U
Annexin I	NP_000691	6.6	38.98	1.98	35	U
Triosephosphate isomerase 1	NP_000356	6.5	26.88	2.41	17	U
Glucose 6-phosphate dehydrogenase isoform α	NP_000393	6.3	59.64	2.43	19	U
Proteolysis						
Proteasome α 1 subunit isoform 2	NP_002777	6.1	29.89	2.43	37	D
Serpin peptidase inhibitor, clade B member 6	NP_004559	5.5	46.99	1.76	20	D
Cell structure and architecture						
Lamin	NP_733822	6.2	69.59	2.43	21	D
Filamin Aα (actin binding protein 280)	NP_001447	6	105.43	2.43	10	D
Lamin A/C isoform 2	NP_005563	6.4	65.19	2.43	28	D
Lamin A/C isoform 1 precursor	NP_733821	6.6	74.48	2.18	21	U
Signaling						
Human rab GDI	NP_001485	5.9	51.21	2.23	13	D
Acidic α 1 syntrophin	NP_003089	6.4	54.3	2.43	16	D
G protein, α activating activity polypeptide, olfactory	NP_002062	6	41.61	2.31	17	U
Transport						
ADP-ribosylation factor domain protein 1 isoform γ	NP_150231	6	62.9	2.43	13	D
Translation						
G elongation factor, mitochondrial 1	NP_079272	6.6	84.31	2.43	11	D
Transcription						
Zinc finger and BTB domain-containing protein 1	NP_055765	6	84.56	2.43	10	D
Interferon regulatory factor 4	NP_002451	6.2	52.62	2.43	18	D
RuvB-like 1 (*E. coli*)	NP_003698	6	50.64	1.8	22	D
Immunity						
Major histocompatibility complex, class I, E precursor	NP_005507	5.5	40.32	2.43	19	D
Protein modification						
Protein-L-isoaspartate *O*-methyltransferase domain-containing protein 2	NP_060727	5.8	41.55	2.43	19	U
Cytokinesis						
Septin 2	NP_004395	6.1	41.75	2.42	42	U
Unclassified biological function						
Chromosome 1 open reading frame 124	NP_114407	6	24.66	2.42	35	D
Protein phosphatase 1, catalytic subunit, β isoform 1	NP_002700	6	38.43	2.37	20	D
Ornithine aminotransferase precursor	NP_000265	5.7	44.97	2.43	19	D
Coiled-coil domain-containing protein 2 (Capillary morphogenesis protein 1: CMG-1)	NP_079379	5.7	69.36	1.66	12	D
Mitofilin	NP_006830	5.6	68.38	2.38	23	D
Ribosomal protein P0	NP_000993	5.7	34.47	2.21	35	D

1 and 24 h of ESP exposure. Immunoblot analysis revealed little or no overexpression at early time-points (1–3 h), except for calpain, which was significantly increased at 3 h, but elevated expression between 9 and 24 h (Fig. 4). This finding was consistent with 2-DE gel image data, regardless of the pH range, indicating that our 2-DE based proteomic tools are effective in identifying proteins regulated by ESP.

DIFFERENTIAL EXPRESSION OF Trx 1 AND Prdx ISOFORMS DURING ESP EXPOSURE

We observed elevated expression of two proteins, specifically, thioredoxin (Trx) 1 and peroxiredoxin (Prdx) 6, detected in the pH 4.5–5.5 and 4–7 gels, respectively (Fig. 5). Since these proteins play divergent roles in biological processes as well as the regulation of cellular redox homeostasis [Nordberg and Arner, 2001; Fujii and Ikeda, 2002], we further analyzed the expression patterns of these proteins during 1–24 h of ESP exposure. Immunoblot analysis revealed significant elevation of Trx 1 expression at 9 h, followed by a further increase at 15 h following ESP exposure (Fig. 6A), confirming the proteomic data. This result raised the possibility of ESP-mediated regulation of 2-cys Prdxs, as Trx is essential for maintaining their activities [Rhee et al., 2001; Hofmann et al., 2002]. In addition, each member of the Prdx family shares a narrow M_r and pI range, which may mask the relative protein abundance on silver-stained 2-D gels. Accordingly, we examined the expression levels of all six Prdx isoforms in cells exposed to ESP between 0 and 24 h by semi-quantitative RT-PCR and immunoblot analysis using isoform-specific primers (Table I) and antibodies, respectively (Fig. 6B,C). In

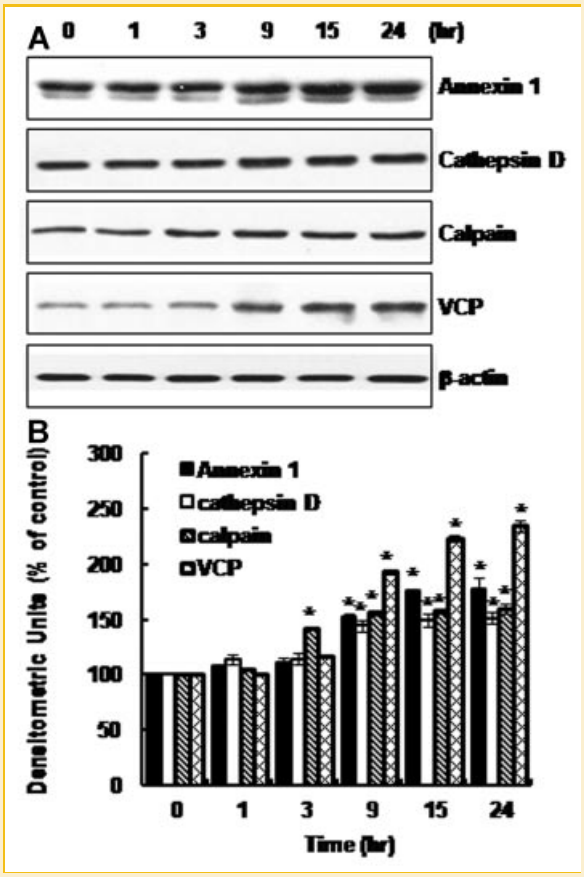

Fig. 4. Expression of annexin 1, cathepsin D, calpain, and VCP in 0–24 h ESP-treated cells, detected with immunoblot analysis. HuCCT1 cells were treated with 800 ng/ml ESP, and harvested at times between 0 and 24 h, followed by immunoblot analysis using specific antibodies for each protein. A: Representative immunoblot. B: Individual data were quantified as densitometric units and normalized with β-actin. Data were expressed as a percentage (relative to the control), and presented as means ± SE of three independent experiments. $^{*}P < 0.05$, compared with the zero time-point.

all six cases, Prdx was expressed at both the mRNA and protein levels in HuCCT1 cells. No changes were evident in the Prdx 1, 4, and 5 mRNA and protein expression patterns during the entire period of ESP exposure whereas Prdx 2, 3, and 6 mRNA and protein levels were induced in a time-dependent manner, indicating transcriptional and translational up-regulation by ESP. A significant increase in Prdx 3 expression was observed as early as 1 h, Prdx 2 at 3 h, and Prdx 6 at 9 h of ESP exposure. Elevated expression was maintained up to 24 h.

INTRACELLULAR ROS GENERATION IN THE PRESENCE OF ESP

The factors responsible for the induction of Trx 1 and several Prdx proteins in ESP-treated cells were further investigated. Since external or internal ROS augmentation is associated with these proteins, we examined whether ESP triggers intracellular ROS generation. CM-H_2-DCFDA, in which reduced DCF is localized to the cytosol and reacts with intracellular oxidants to become fluorescent, was employed as an oxidation-sensitive fluorescent probe to monitor ROS generation within cells. DCF fluorescence was measured using a fluorometer or microscope. Fluorescence levels were significantly elevated in proportion with the ESP concentration (Fig. 7A). Treatment with 800 ng/ml ESP resulted in elevated DCF intensity, with the most significant increase at 9 h of incubation. Subsequently, the intensity of cellular fluorescence gradually declined between 15 and 24 h, but was still stronger than that of the untreated control (Fig. 7B). To confirm that ESP are responsible for ROS generation, cells were preincubated with a ROS scavenger (NAC), followed by exposure to ESP for 9 h. NAC significantly inhibited ROS generation in a dose-dependent manner, leading to almost complete blockage at a concentration of 20 mM (Fig. 7C). Treatment with NAC attenuated up-regulation of Prdx 2 and 6 by ESP (Fig. 7D), clearly indicating that ESP-mediated ROS contribute to induction of these Prdx expressions. Interestingly, increased Prdx 3 expression was maintained, even in the presence of NAC. NAC-dysregulated Prdx 3 may result from its differential distribution within cells. While Prdx 2 and 6 are mainly localized in the cytosol, Prdx 3 is present in mitochondria that consume 85% of oxygen in cells and continuously generate ROS as by-products. Thus, consecutive Prdx 3 expression is required to perform a general protective role in these organelles. Moreover, we cannot rule out the possible involvement of additional signals from ESP for stimulation of Prdx 3 expression.

DISCUSSION

Pathogenesis of *C. sinensis* infestation is a complex process involving both mechanical and chemical irritation of the bile ducts and surrounding liver tissues. The former is caused by direct contact of parasites with bile duct epithelium, and the latter by their ESP [Vatanasapt et al., 1999]. In particular, ESP from liver flukes is potent inducers of various pathophysiologic responses in host cells [Cervi and Masih, 1997; Thuwajit et al., 2004; Serradell et al., 2007; Kim et al., 2008; Pak et al., 2009]. Therefore, we performed experiments using a cell culture system (human cholangiocarcinoma cell line, HuCCT1) with *C. sinensis* ESP to analyze the expression patterns of host cellular proteins. To our knowledge, this is the first attempt to describe global changes in protein expression of host cells in response to *C. sinensis* ESP at the proteome level.

The proteomic approach using 2-DE for protein expression changes and mass spectrometry for identification revealed that 83 host cellular proteins were modulated by *C. sinensis* ESP (Table II). The identified proteins were classified into 18 functional categories involving various biological processes, suggestive of multiple roles of ESP in host cells. In particular, proteins involved in signal transduction and metabolism occupied the highest portion among biological processes, which was similar to our previous transcriptome profiles [Pak et al., 2009]. Although it is difficult to generalize the pathologic signaling pathways mediated by ESP, these data show the valuable evidences of the protein level changes, and furthermore these differentially expressed proteins may be potential targets for pathophysiologic effects of *C. sinensis* ESP or even infection on host cells. Therefore, this proteome profiling provides the resources for further investigation to characterize various proteins involved in ESP-controlled molecular mechanisms and

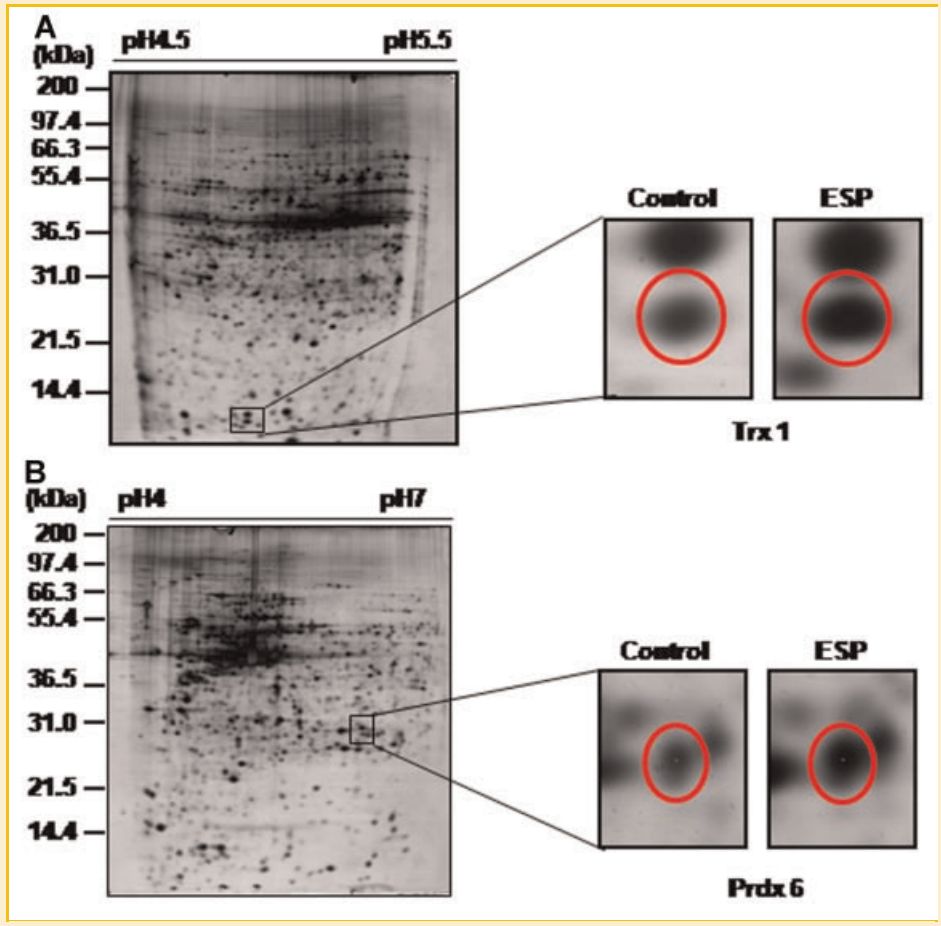

Fig. 5. 2-DE maps for the positions of Trx 1 (A) and Prdx 6 (B) spots. The right sides display the comparative magnified regions between cells treated with PBS (control) and ESP (ESP) for 24 h. The pI and M_r values of Trx 1 and Prdx 6 obtained from 2-DE gels were similar to their theoretical values.

signal transduction in an in vitro model system, which is similar to that of *C. sinensis* infection in vivo.

Of particular interest was that ESP treatment resulted in up-regulation of Trx 1 and Prdx 6 expression (Fig. 5), as ESP of *C. sinensis* and *O. viverrini* are potential promoters for the development of cholangiocarcinoma [Thuwajit et al., 2004; Kim et al., 2008] and Trx 1 and Prdx 6 expression patterns are significantly associated with tumor progression. Trx 1 is an oxidoreductase containing two redox-active cysteine residues within a conserved active center, which can be oxidized to form intramolecular disulfide bonds. Reduction of oxidized Trx is catalyzed by Trx reductase with NADPH as an electron donor. Specific protein disulfide targets for reduced Trx 1 include ribonucleotide reductase, protein disulfide-isomerase and several transcription factors, including p53, NF-κB, and AP1. Trx 1 is also capable of removing H_2O_2, particularly when coupled with either methionine sulfoxide reductase or 2-cys Prdx proteins [Nordberg and Arner, 2001]. Prdx 6 is the only mammalian 1-cys member of the Prdx superfamily, which function as thiol-dependent peroxidases utilizing active cysteine residues as the catalytic center to reduce a wide range of peroxides [Rhee et al., 2001; Hofmann et al., 2002]. Whereas Prdx 1-5 contain two reactive cysteines (thus named as 2-cys Prdx) and use Trx as a reductant, Prdx 6 has a single redox-active cysteine and employs glutathione as an electron donor through glutathione *S*-transferase π-mediated reduction [Manevich et al., 2004; Ralat et al., 2006]. Trx 1 and Prdx 6 levels were increased in various types of malignant human tumors, suggesting that their overexpression is strongly associated with cancer development and progression [Kinnula et al., 2002; Quan et al., 2006; Powis and Kirkpatrick, 2007]. This theory is supported by the finding that Trx 1 inhibits apoptosis of cancer cells by binding to apoptosis signal-regulating kinase-1 (Ask-1) or the tumor suppressor, PTEN. Moreover, an endogenous blocker of Trx 1-binding protein (TXNIP), a tumor suppressor and metastasis inhibitor, competes with Trx 1 for binding to Ask-1, rendering cells susceptible to stress-induced apoptosis [Powis and Kirkpatrick, 2007]. Prdx 6-transfected breast cancer cells grow, invade and metastasize more readily than control cells, both in vitro and in vivo, partially through modulation of invasion-related gene expression [Chang et al., 2007].

We noticed that all Prdx isoforms were not responding to ESP (Fig. 6). One possible explanation is that individual Prdx proteins exhibit distinct tissue expression and subcellular localization as well as different responses to various stimuli, which are attributable to their independent physiologic functions. In addition to their primary

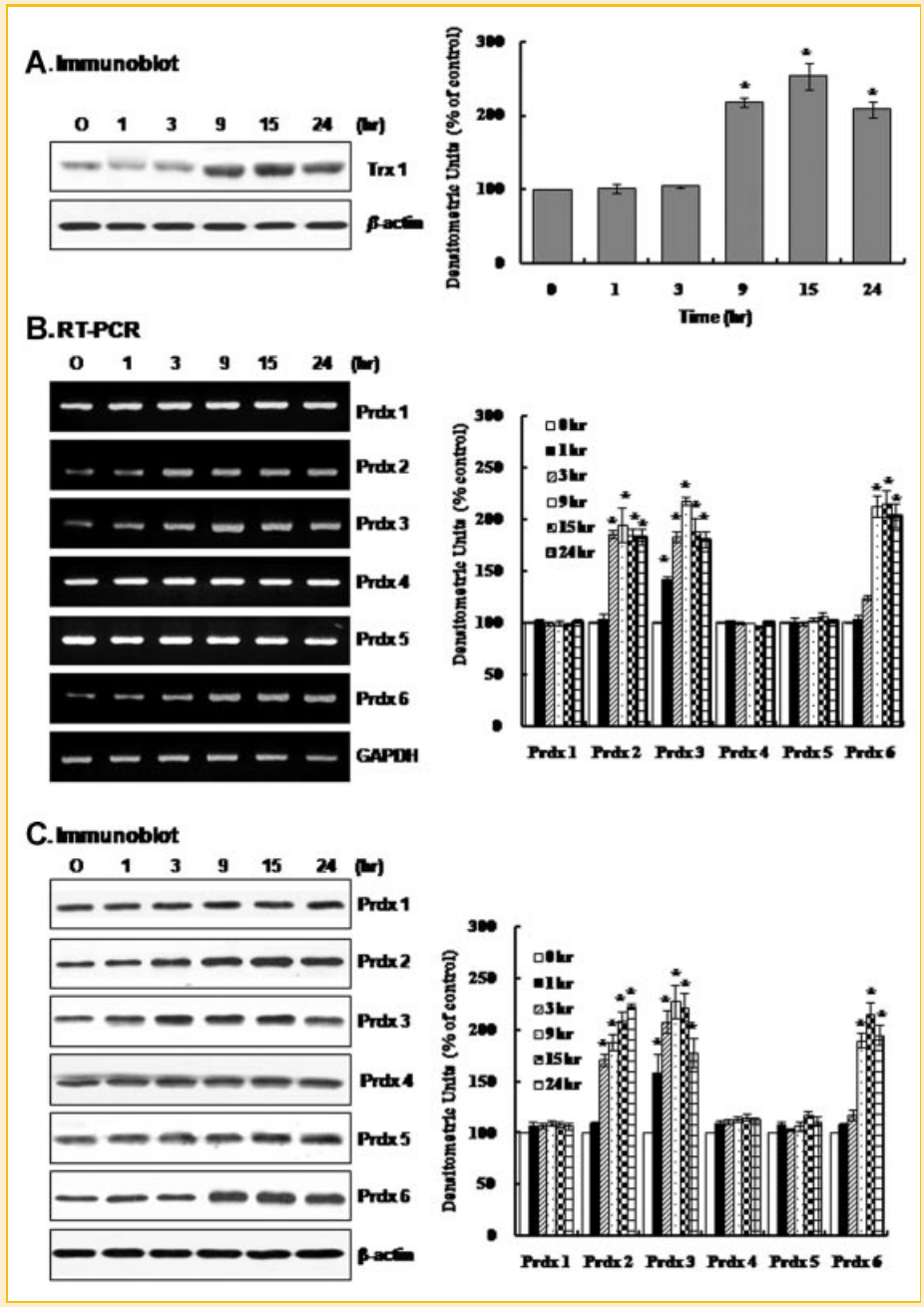

Fig. 6. Effect of ESP on Trx 1 protein, and Prdx 1–6 mRNA and protein expression. HuCCT1 cells were treated with 800 ng/ml ESP, harvested at specific times between 0 and 24 h, and subjected to expression analyses. A: Representative immunoblot of Trx 1 protein. B: Semi-quantitative RT-PCR of Prdx 1–6 mRNA. C: Representative immunoblots of Prdx 1–6. Individual data were quantified as densitometric units, and normalized with β-actin for protein or GADPH for mRNA, respectively. Data in graphs are shown as a percentage (relative to zero time, control), and presented as means ± SE of three independent experiments. $^{*}P < 0.05$, compared to the zero time-point in the same group.

functions as antioxidant enzymes, Prdx proteins are implicated in cell proliferation, differentiation, immune response, control of apoptosis, and processes involving redox signaling [Fujii and Ikeda, 2002; Immenschuh and Baumgrart-Vogt, 2005; Rhee et al., 2005]. Specific members of the Prdx protein family are highly expressed in human cancer tissues, including Prdx 3–5 in breast carcinoma [Karihtala et al., 2003], and Prdx 1, 2, 4, and 6 in lung cancer [Lehtonen et al., 2004]. Cancer type-specific differences in the expression of each Prdx isoform were correlated with tumor histopathology, potential effects on tumor progression, and patient clinical data. These studies further suggest that the Prdx increase occurs due to increased ROS production in carcinomatous tissue, thereby manipulating a dynamic redox change in the tumor microenvironment supporting proliferation and malignant progression.

Consistent with our results (Fig. 7), ROS generation mediated by liver fluke has been reported, both in vitro and in vivo. The

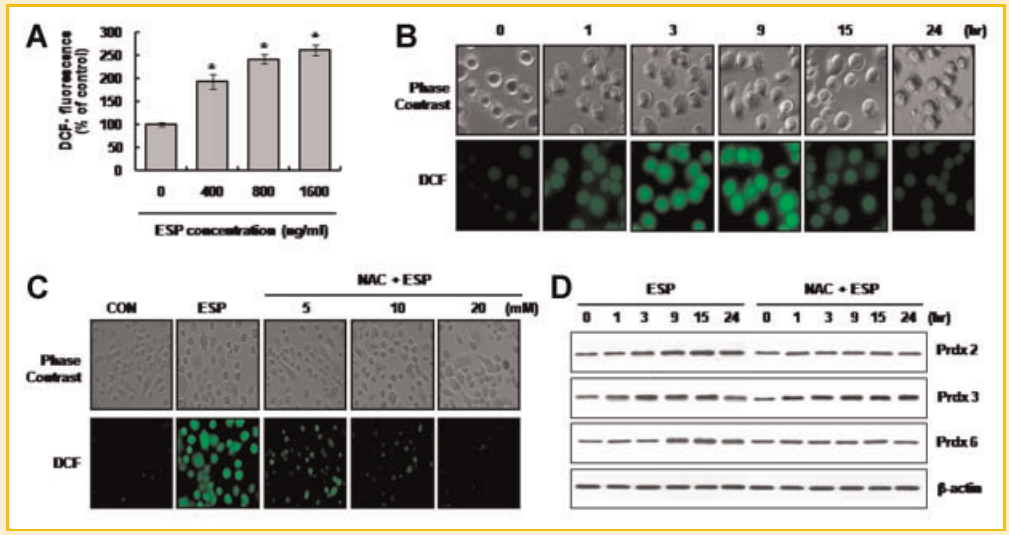

Fig. 7. Detection of ESP-mediated ROS generation with DCF fluorescence and its effect on expression of Prdx 2, 3, and 6. A: HuCCT1 cells were treated with various concentrations of ESP (400–1,600 ng/ml) for 3 h, and DCF fluorescence measured with a spectrofluorometer. Each dataset represents the relative percentage of the untreated control. Values are presented as means ± SE of three independent experiments. $^{*}P < 0.05$, compared to untreated control. B: HuCCT1 cells were treated with 800 ng/ml ESP for 0–24 h, and fluorescent images captured using a fluorescence microscope with a single rapid scan and identical parameters. C: HuCCT1 cells were preincubated with 5–20 mM NAC for 1 h, followed by treatment with 800 ng/ml ESP for 9 h. Subsequently, DCF fluorescence was measured, as described in panel B. D: The conditions for ESP treatment were essentially identical to those specified for panel C, except for preincubation with 10 mM NAC and ESP exposure times. Cells were harvested for immunoblot analysis of Prdx 2, 3, and 6 levels. The quantity of protein applied was normalized with β-actin as a loading control.

suppressive effect of *F. hepatica* ESP on the proliferative response of rat splenocytes to mitogens was partially attenuated by supplying antioxidant enzymes, such as superoxide dismutase (SOD) and catalase, suggesting that the ESP triggers ROS release in host cells leading to immunosuppression for parasite survival [Cervi and Masih, 1997]. Moreover, nitric oxide (NO) was overexpressed in the liver of hamsters infected with *O. viverrini* via activation of inducible nitric oxide synthase (iNOS), leading to nitroso compound formation in the nuclei of small inflammatory cells and epithelia of bile ducts. As a result, nitrative and oxidative DNA damage possibly participating in the initiation and/or promotion of cholangiocarcinoma carcinogenesis was enhanced [Pinlaor et al., 2004]. Intracellular ROS are generated by multiple mechanisms, such as mitochondrial respiration, ionizing radiation, and enzyme reactions, including the NADPH oxidase system, xanthine oxidase, lipoxygenase and cyclooxygenase. While ROS act as a second messenger participating in signal transduction, differentiation, apoptosis, and modulation of transcription factors at physiological concentrations, excess ROS production causes serious cellular injuries and contributes to the pathogenesis of numerous human diseases [Thannickal and Fanburg, 2000]. In view of the proposed function of *C. sinensis* ESP (focusing on ROS stimulation in host cells) and high affinity of Prdx proteins for ROS, it is tempting to speculate that the Prdx system is involved in a variety of cellular processes via modulating the concentration of intracellular ROS existing either as toxic by-products or second messengers. In particular, the antiapoptotic features of Prdxs by impending oxidative stress provide a growth advantage to tumor cells during carcinogenesis.

In conclusion, clonorchiasis induces chronic irritation and prolonged inflammation in the bile duct epithelium and surrounding liver tissues, subsequently leading to the development of cholangiocarcinoma as a result of direct contact with *C. sinensis* worms and their ESP. Among these, Trx 1 and several Prdx isoforms are associated with the potential role of ESP as a carcinogen, although detailed functional tests with these proteins are yet to be performed. Comprehensive identification of *C. sinensis* ESP proteins and their characterization is necessary to establish the signal pathways underlying parasite-host interactions. The current findings extend our understanding of the molecular mechanisms of *C. sinensis* infection, and provide possible strategies to circumvent clonorchiasis-associated disease.

ACKNOWLEDGMENTS

We thank Dr. Jung Won Ju for technical assistance with the preparation of *C. sinensis* ESP, Dr. Young Yil Bahk for advice regarding 2-DE, Sung-Ha Park for assistance with proteome data analysis, and Hye Mi Lee for figure revision.

REFERENCES

Blacktock WP, Weir MP. 1999. Proteomics: Quantitative and physical mapping of cellular proteins. Trends Biotechnol 17:121–127.

Cervi L, Masih DT. 1997. Inhibition of spleen cell proliferative response to mitogens by excretory-secretory antigens of *Fasciola hepatica*. Int J Parasitol 27:573–579.

Chang XZ, Li DQ, Hou YF, Wu J, Lu JS, Di GH, Jin W, Ou ZL, Shen ZZ, Shao ZM. 2007. Identification of the functional role of peroxiredoxin 6 in the progression of breast cancer. Breast Cancer Res 9:R76.

Choi D, Lim JH, Lee KT, Lee JK, Choi SH, Heo JS, Jang KT, Lee NY, Kim S, Hong ST. 2006. Cholangiocarcinoma and *Clonorchis sinensis* infection: A case-control study in Korea. J Hepatol 44:1066–1073.

Crompton DW. 1999. How much human helminthiasis is there in the world? J Parasitol 85:397–403.

Fujii J, Ikeda Y. 2002. Advances in our understanding of peroxiredoxin, a mutifunctional, mammalian redox protein. Redox Rep 7:123–130.

Hofmann B, Hecht H, Flohe L. 2002. Peroxiredoxins. Biol Chem 383:347–364.

Hong SJ, Kim TY, Gan XX, Shen LY, Sukontason K, Sukontason K, Kang SY. 2002. *Clonorchis sinensis*: Glutathione S-transferase as a serodiagnostic antigen for detecting IgG and IgE antibodies. Exp Parasitol 101:231–233.

Immenschuh S, Baumgrart-Vogt E. 2005. Peroxiredoxins, oxidative stress, and cell proliferation. Antioxid Redox Signal 7:768–777.

Jefferies JR, Campbell AM, van Rossum AJ, Barrett J, Brophy PM. 2001. Proteomic analysis of *Fasciola hepatica* excretory-secretory products. Proteomics 1:1128–1132.

Ju JW, Joo HN, Lee MR, Cho SH, Cheun HI, Kim JY, Lee YH, Lee KJ, Sohn WM, Kim DM, Kim IC, Park BC, Kim TS. 2009. Identification of a serodiagnostic antigen, legumain, by immunoproteomic analysis of excretory-secretory products of *Clonorchis sinensis* adult worms. Proteomics 9:3066–3078.

Kang TH, Yun DH, Lee EH, Chung YB, Bae YA, Chung JY, Kang I, Kim J, Cho SY, Kong Y. 2004. A cathepsin F of adult *Clonorchis sinensis* and its phylogenetic conservation in trematodes. Parasitology 128:195–207.

Karihtala P, Mantyniemi A, Kang SW, Kinnula VL, Soini Y. 2003. Peroxiredoxins in breast carcinoma. Clin Cancer Res 9:3418–3423.

Kim YJ, Choi MH, Hong ST, Bae YM. 2008. Proliferative effects of excretory/secretory products from *Clonorchis sinensis* on human epithelial cell line HEK293T via regulation of the transcription factor E2F1. Parasitol Res 102:411–417.

Kinnula VL, Lehtonen S, Sormunen R, Kaarteenaho-Wiik R, Kang SW, Rhee SG, Soini Y. 2002. Overexpression of peroxiredoxins I, II, III, V, and VI in malignant mesothelioma. J Pathol 196:316–323.

Lehtonen ST, Svensk AM, Soini Y, Paakko P, Hirvikoski P, Kang SW, Saily M, Kinnula VL. 2004. Peroxiredoxins, a novel protein family in lung cancer. Int J Cancer 111:514–521.

Li S, Chung BS, Choi MH, Hong ST. 2004. Organ-specific antigens of *Clonorchis sinensis*. Korean J Parasitol 42:169–174.

Manevich Y, Feinstein SI, Fisher AB. 2004. Activation of the antioxidant enzyme 1-cys peroxiredoxin requires glutathionylation mediated by heterodimerization with π-GST. Proc Natl Acad Sci USA 101:3780–3785.

Nordberg J, Arner ES. 2001. Reactive oxygen species, antioxidants, and the mammalian thioredoxin system. Free Radic Biol Med 31:1287–1312.

Pak JH, Kim D, Moon JH, Nam JH, Kim JH, Ju JW, Kim TS, Seo SB. 2009. Differential gene expression profiling in human cholangiocarcinoma cells treated with *Clonorchis sinensis* excretory-secretory products. Parasitol Res 104:1035–1046.

Papachristou GI, Schoedel KE, Ramanathan R, Rabinovitz M. 2005. *Clonorchis sinensis*-associated cholangiocarcinoma: A case report and review of the literature. Digest Dis Sci 50:2159–2162.

Park JW, Kim S, Lim KJ, Simpson RJ, Kim YS, Bahk YY. 2006. A proteomic approach for unraveling the oncogenic H-Ras protein networks in NIH/3T3 mouse embryonic fibroblast cells. Proteomics 6:1175–1186.

Pinlaor S, Hiraku Y, Ma N, Yongvanit P, Semba R, Oikawa S, Murata M, Sripa B, Sithithaworn P, Kawanishi S. 2004. Mechanism of NO-mediated oxidative and nitrative DNA damage in hamsters infected with *Opisthorchis viverrini*: A model of inflammation-mediated carcinogenesis. Nitric Oxide 11:175–183.

Powis G, Kirkpatrick LD. 2007. Thioredoxin signaling as a target for cancer therapy. Curr Opin Phamacol 7:392–397.

Quan C, Cha EJ, Lee HL, Han KH, Lee KM, Kim WJ. 2006. Enhanced expression of peroxiredoxin I and VI correlates with development, recurrence and progression of human bladder cancer. J Urol 175:1512–1516.

Ralat LA, Manevich Y, Fisher AB, Colman RF. 2006. Direct evidence for the formation of a complex between 1-cys peroxiredoxin and glutathione S-transferase π with activity changes in both enzymes. Biochemistry 45:360–372.

Rhee SG, Kang SW, Chang TS, Jeong W, Kim K. 2001. Peroxiredoxin, a novel family of peroxidases. IUBMB Life 52:35–41.

Rhee SG, Chae HZ, Kim K. 2005. Peroxiredoxins: A historical overview and speculative preview of novel mechanisms and emerging concepts in cell signaling. Free Radic Biol Med 38:1543–1552.

Rim HJ. 2005. Clonorchiasis: An update. J Helminthol 79:269–281.

Serradell MC, Guasconi L, Cervi L, Chiapello LS, Masih DT. 2007. Excretory-secretory products from *Fasciola hepatica* induce eosinophil apoptosis by a caspase-dependent mechanism. Vet Immunol Immunopathol 117:197–208.

Shim JH, Danielpour D, Lee C, Kim YS, Bahk YY, Yoo TK. 2004. Proteome profile changes during transdifferentiation of NRP-152 rat prostatic basal epithelial cells. Mol Cells 17:108–116.

Shim JH, Kim YS, Bahk YY. 2006. Proteome profile changes that are differentially regulated by lipid and protein phosphatase activities of tumor suppressor PTEN in PTEN expressing U-87 MG human glioblastoma cells. Proteomics 6:81–93.

Thannickal VJ, Fanburg BL. 2000. Reactive oxygen species in cell signaling. Am J Physiol Lung Cell Mol Physiol 279:L1005–L1028.

Thuwajit C, Thuwajit P, Kaewkes S, Sripa B, Uchida K, Miwa M, Wongkham S. 2004. Increased cell proliferation of mouse fibroblast NIH-3T3 in vitro induced by excretory/secretory product(s) from *Opisthorchis viverrini*. Parasitology 129:455–464.

Vatanasapt V, Sripa E, Sithithaworn P, Mairiang P. 1999. Liver flukes and liver cancer. Cancer Survey 33:313–343.

Watanapa P, Watanapa WB. 2002. Liver fluke-associated chrolangiocarcinoma. Br J Surg 89:962–970.

Yan JX, Wait R, Berkelman T, Harry RA, Westbrook JA, Wheeler CH, Dunn MJ. 2000. A modified silver staining protocol for visualization of proteins compatible with matrix-assisted laser desorption/ionization and electrospray ionization-mass spectrometry. Electrophoresis 21:3666–3672.